GMR EFFECT IN ELECTRODEPOSITED Cu/CoNi(Cu) MULTILAYERS

P.L. Cavallotti[a], D. Manara[a], R. Vallauri[a], A.Vicenzo[a], J.Machado da Silva[b], M.A. Sà[b]

[a] Politecnico di Milano - Dip. Chimica Fisica Applicata
Via L.Mancinelli,7 20131 - Milan - ITALY
[b] Centro de Física, Universidade do Porto
R. do Campo Alegre, 687P-4150 Porto - PORTUGAL

ABSTRACT

GMR effect was studied in Cu/CoNi(Cu) superlattices prepared by electrodeposition from a single sulphamate bath containing *Rochelle* salt, under galvanostatic control at pH 6.40. The influence of substrate, single layers thickness, heat treatment and additives was investigated in details.
GMR measurements were performed at room temperature; no correction was made for substrate contribution. Multilayers structure and surface morphology were characterised by X-ray diffraction, Scanning Electron Microscopy and EDS microanalysis.
Multilayers with interesting GMR% values, high sensitivity and very low saturation magnetic field, Middle Height Width and coercivity were obtained. These properties are of the utmost importance in view of possible applications in the field of magnetic storage and sensors.

INTRODUCTION

Much attention was given to the Giant Magnetoresistance (GMR) effect since the first observation of large resistance changes in Fe/Cr (1), Co/Cu multilayers and other metallic multilayer systems; GMR was also observed in Co-Cu granular alloy films produced either by sputtering or by electrodeposition (2-6).

With ElectroChemical Deposition (ECD) it is possible to produce multilayers or modulated films of suitable composition and thickness by adjusting and controlling the operation conditions. ECD process is less expensive than a vapour-phase deposition technique because a vacuum system is not required; furthermore with ECD we operate at room temperature and it is possible to obtain thin films onto substrates of any shape.

This paper deals with the GMR effect in ECD CoNi(Cu)/Cu multilayers. The electrodeposition conditions as well as the substrate influence were studied in details. The importance of Cu and Co layers thickness and the effect of additives on the growth habit and GMR performance of the multilayers were also considered. Multilayer thermal stability was tested by vacuum heat treatments (250°C, 1h).

EXPERIMENTAL

The deposition was carried out from a single electrolyte (7,8) containing Co, Ni, Cu sulphamates and Rochelle salt ($NaKC_4H_4O_6$). Table I gives bath compositions and plating conditions. The electrolytes were prepared with analytical grade reagents and double distilled water. The solutions were purified by charcoal treatment and deaerated by nitrogen bubbling. The copper concentration in the electrolyte was adjusted to minimise the copper content in the magnetic layers.

Figure 1 shows the potentiodynamic polarisation curves of the baths investigated, all obtained with gentle stirring, at pH=6.40 and T=48°C, on Cu substrates. Potentiodynamic runs were performed at 0.5 mV/s with a *Model 273A EG&G PRINCETON* potentiostat-galvanostat. The potential range at which copper and CoNi(Cu) deposition occurs is clearly defined in particular in the case of bath 3, containing Sodium Hypophosphite. The CoNi(Cu) limiting current density is 7÷9 mA/cm^2.

A "triple" current pulse technique (9,10) was used. A cycle consisted of a long (4-60 s) low current pulse (copper deposition step); a short (1-3 s) high current pulse, during which essentially cobalt and nickel are deposited; a short (0.1 s) off time pulse. Copper was deposited at 0.5 mA/cm^2; cobalt-nickel alloy at 5-6 mA/cm^2. The ferromagnetic layers are characterised by about 20:1 Co to Ni ratio and about 30 at. % Cu content. An *AMEL System 5000* potentiostat-galvanostat was used for the multilayer deposition.

The Cu/CoNi(Cu) multilayers were deposited onto silicon wafers, coated with following sputtered seed-layers: A)$Ni_{80}Fe_{20}$(100nm); B) SiO_2(100nm)+$Ni_{80}Fe_{20}$ (20nm);C) Cr(20nm) with Au ECD flash; D) ITO(*Indium Tin Oxide* -160nm) with Au ECD flash; E) SiO_2+Cr(70nm) with Au ECD flash.

Microstructure, composition and morphology were characterised by X-ray diffraction, EDS microanalysis and Scanning Electron Microscopy (SEM).

The magnetoresistance ratio is measured with respect to the resistance in the highest applied magnetic field. The saturation magnetoresistance is the highest resistance in the experimental field, normalised with respect to the resistance at the highest applied magnetic field, and it is defined by $\Delta R/R(\%)=(R(H)-R(H_{max}))/R(H_{max})$.

GMR ratio [%], Middle Height Width [Oe], coercivity [Oe] and sensitivity [%/kOe] were measured at room temperature with a low-frequency lock-in amplifier using a standard four contacts technique and applying a magnetic field parallel to an AC current flowing through the sample. No correction was made for substrate contribution.

RESULTS

Substrate influence

Several substrates were tested in order to clarify the influence of roughness, coarseness and electrical conductivity of the material to be plated on the whole set of GMR and magnetic properties of multilayers. In general, the brighter, more uniform and smoother

was the substrate, the higher were the maximum GMR% change and sensitivity and the lower were the coercivity and Middle Height Width.

With substrates B, D and E the highest GMR values were achieved.

Substrate A short-circuited the multilayers completely and gave the lowest GMR effect.

Substrate C gave low GMR effect because of its high electrical conductivity and roughness. In this case the undesirable effect of substrate roughness could be overcome by depositing a thin bright Nickel ECD film before ML deposition. The GMR effect was increased, giving results near to those obtained with substrate B, and this could be ascribed to the improvement in the ML compositional modulation. We could observe the appearance of *satellite peaks* on both sides of fcc (111) and fcc (200) reflections in XRD patterns. Figure 2 shows the XRD pattern of a sample with 8nm expected modulation length.

Satellite peaks are observed when a "superlattice" structure occurs over the periodicity of the crystalline lattice, as it is the case of our multilayer. Satellite peaks are observed on both sides of the main crystal lattice diffraction peaks, at diffraction angles (θ^+, θ^-) according to:

$$\frac{2 \cdot sin\left(J^{\pm}\right)}{l_x} = \frac{1}{d} \pm \frac{n}{l} \qquad [1]$$

where Λ is the superlattice modulation length, n is the satellite peaks order, d is the distance between crystalline planes and λ_x the X-ray wavelength.
The experimental modulation length corresponding to the satellite peaks found in the XRD pattern (7,87 nm and 8,04 nm respectively) is in good agreement with the expected value (8 nm).

Figures 3 and 4 show the SEM micrographs of two $[Cu(5nm)/CoNi(Cu)(3nm)]_{40}$ multilayers, deposited onto substrate B in the absence and in the presence of a thin bright Ni ECD layer, respectively. Surface roughness and grain size are low when a bright Ni ECD flash was applied before ML deposition. Table II gives the GMR values for these two multilayers. The improved modulation obtained in the presence of a thin bright Ni ECD layer gave an increased $\Delta R/R_{MAX}$% and sensitivity as well as a decreased coercivity. Figure 5 shows a comparison between the GMR curves of the two samples.

Very interesting results were obtained by electrodeposition onto substrates D and E. Substrate D (ITO) is a Si wafer on which a 160 nm film of Indium Oxide doped with Tin was deposited. Onto this substrate an Au ECD flash had to be deposited because of its low electrical conductivity. ITO layer shows a cubic Indium Oxide In_2O_3 crystalline structure with (222) preferred orientation; the surface shows a certain roughness. Multilayers grown onto this substrate also show a coarse surface with large grain size. Figure 6 shows a SEM micrograph of a $[Cu(7.5nm)/CoNi(Cu)(3nm)]_{40}$ sample, deposited onto substrate D. Substrate and deposit coarseness are evident. The best GMR results were obtained depositing onto this substrate. $\Delta R/R_{MAX}$% had a maximum value of 6.90%. This was also a consequence of low conductivity of the substrate.

Substrate E was a 70 nm Cr layer sputtered onto a SiO_2 layer, with a final Au ECD

flash to overcome the problem of possible Cr oxidation; the surface was smooth and uniform. Multilayers grown onto this substrate showed low surface roughness; interfaces with good definition between the layers and fine grain size could be obtained. Figure 7 shows a SEM micrograph of a $[Cu(7.5nm)/CoNi(Cu)(3nm)]_{40}$ ML electrodeposited onto this substrate. Multilayers grown onto substrate E ($Si+SiO_2+Cr(70nm)$), with a non-conductive SiO_2 layer, showed higher GMR effect than those grown onto substrate C with a very thin Cr layer(20nm).

Substrate B is a Si wafer with 100 nm SiO_2 + 20 nm $Ni_{80}Fe_{20}$ seed layer. Its surface is as smooth as that of substrate E. Multilayers electrodeposited onto this substrate show very low coercivity, down to about 40 Oe.

Table III gives the comparison between GMR measurements of different multilayers grown on substrates B,D and E respectively. Figure 8 shows a comparison between GMR curves of three $[Cu(5nm)/CoNi(Cu)(3nm)]_{40}$ samples, grown on substrate B,D, and E respectively.

Crystal structure of electrodeposited superlattices grown onto different substrates was analysed by X-ray diffraction (XRD). Substrate (see fig.9) does not have a significant influence on multilayers crystalline structure. XRD patterns of superlattices having the same compositional modulation but grown onto different substrates, do not present any significant difference in crystal orientation. However, the substrate has a strong influence on the interfaces structure and morphology, and, in this way, it greatly affects the coercivity and the GMR properties.

The influence of single layers thickness

A reproducible GMR effect increase was observed at Cu layers thickness higher than 3.5 nm. Figures 10 and 11 show GMR ratio and Middle Height Width as a function of copper layer nominal thickness on Si+Cr(20nm)+Au ECD flash substrate.

The highest GMR values were found for Cu layer thickness ranging from 5 to 8 nm. Increasing Cu layer thickness, GMR ratio increased, while the ratio of fcc(111)/fcc(200) XRD peak intensity decreased. The same correlation between GMR and copper thickness was observed for multilayers electrodeposited onto different substrates. In figure 12 the results concerning samples deposited onto Si/ITO substrates are shown.

The maximum percentage change in GMR does not appear to oscillate at increasing t_{Cu}, as Alper et al (11) already noticed for electrodeposited Cu/CoNi(Cu) multilayers. However, more data points would be needed to exclude such possibility completely.

These findings could be related to the presence of undulating rather than flat interfaces between adjoining layers, or to the presence of regions where contact between successive ferromagnetic layers could occur. At low t_{Cu} (<3.5 nm) interface roughness could result in some regions of the superlattices antiferromagnetically coupled, even when the average Cu thickness could favour ferromagnetic exchange coupling, and vice versa (12). Such irregular magnetic coupling could be responsible for the strong suppression of the GMR observed at small t_{Cu}, as Hua, Lashmore et al (13) already pointed out. For t_{Cu} higher than 4 nm, GMR curves are consistent with weak antiferromagnetic coupling and good layer definition improves GMR effect. For t_{Cu} higher than 3.5nm, GMR peaks Middle Height Width attained a steady value of 160 Oe in MLs grown onto Si+Cr+Au ECD flash and of about 250 Oe for those grown onto Si+ITO substrate.

In MLs having t_{Cu} lower than 3.5÷4 nm interesting GMR% values were observed only with a high number of layers; this could be attributed at low thickness to the increase of substrate short-circuit effect. Figure 13 shows the GMR curve of a $[Cu(1.2nm)/CoNi(Cu)(3nm)]_{255}$ sample grown onto $Si+SiO_2+Cr+Au$-ECD-flash substrate.

In conclusion, in samples with t_{Cu} lower than 3.5 nm we could not observe high GMR effect, because of the bad layer interfacing, not permitting good AF coupling, and because of the electric and magnetic influence of the substrate.

Another important factor affecting electrodeposited superlattices is their crystal orientation. Figures 14 and 15 show the comparison between XRD patterns at increasing t_{Cu} for samples grown onto Si+Cr+Au ECD flash and Si+ITO+Au substrates. Increasing t_{Cu} MLs show a decrease of fcc(111)/fcc(200) XRD peak intensity ratio and an increase of the GMR effect. A high GMR effect with a low PO is in agreement with published results (14).

Magnetoresistive and magnetic properties increasing CoNi(Cu) ferromagnetic layer thickness (t_{CoNi}) were also studied. GMR effect increased with t_{CoNi} and showed a maximum at 3nm. The CoNi(Cu) thickness at which the GMR maximum occurred was unaffected by Cu-layer thickness and substrate. Nominal thickness do not take into account possible change in current efficiency, and the actual CoNi(Cu) layers thickness could be lower than 3nm. These results are also in agreement with published results.

Heat Treatment influence

Thermal stability of multilayers grown onto $Si+SiO_2(100nm)+Ni_{80}Fe_{20}(20nm)$ and onto Si+Cr(20nm)+Au-ECD flash at increasing copper layer thickness (t_{Cu}) was studied. Figure 16 shows the GMR% vs. t_{Cu} for some of these superlattices before and after a 250°C-1h vacuum heat treatment (H.T.). For t_{Cu} lower than 3÷4 nm GMR effect increased and coercivity decreased after H.T. At low t_{Cu}, a partial recrystallisation is inferred, involving layer structure improvement and GMR effect increase. At high t_{Cu} H.T. favoured copper diffusion into the magnetic layers with GMR effect decrease. However, these effects are quite modest, permitting to consider thermal stability as fairly good. Figure 17 shows a comparison between GMR curves of the $[Cu(5nm)/CoNi(Cu)(3nm)]_{40}$ sample before and after 250°C-1h vacuum heat treatment.

Effect of additives to the bath on GMR

The additions to our standard electrolyte of Sodium Hypophosphite (0.06mol/l-Bath3) and of a Thiocompound (5ppm-Bath 4) were tested.

Sodium Hypophosphite allowed a better definition of the cobalt and nickel potential range and increased fcc(111) preferred crystal orientation, especially at low copper layer thickness (see figure 18). Enhancing (111) P.O. a decreased GMR effect was observed in agreement with W. Schwarzacher and D. S. Lashmore results (14).

Thiocompound addition was studied in order to promote deposit nucleation and growth, because of selective sulphur inhibition on copper deposition. Copper layer definition was improved, as shown in figures 19 and 20 reporting SEM micrographs of two copper films electrodeposited at 0.5 mA/cm^2 in the absence (Bath 1) and in the presence (Bath 4) of the Thiocompound. As a consequence, $\Delta R/R\%$ and sensitivity increased while coercivity decreased. Table IV shows a comparison between GMR measurements of four $[Cu(5nm)/CoNi(Cu)(3nm)]_{40}$ multilayers electrodeposited from bath 1 and 4. Figures 21 and 22 show samples II and IV GMR curves respectively. These measurements were performed at room temperature, using the Van Der Pauw technique and applying a magnetic field parallel to the current circulating through the multilayer. The substrate contribution was not taken into account.

CONCLUSIONS

At high t_{Cu} the shape of GMR curves is consistent with t_{Cu} being large enough for the magnetic layers to be weakly coupled. Quite uncoupled magnetic layers could switch their magnetisation direction at slightly different values of the applied magnetic field, leading to non-parallel alignment of successive layers and hence GMR peaks close to $\pm H_C$, where H_C is the superlattice coercivity (14). The lack of strong coupling would explain why it was possible to observe a large GMR change in a relatively small applied field and hence high sensitivity and low saturation magnetic field.

At low t_{Cu} the following are responsible for the relatively low GMR effect: defects resulting from cobalt dissolution during copper deposition; the high Cu content in CoNi(Cu) layers and the presence of regions of contact between successive ferromagnetic layers.

Summing up, in the present work we electrodeposited multilayers showing:

- GMR% values higher than 4%, with a maximum of ~7%;
- Middle height width lower than 160 Oe, with a minimum of 120 Oe;
- Sensitivity higher than 35 %/kOe, with a maximum of 70 %/kOe;
- Coercivity values about 40 - 50 Oe, with a minimum of 25 Oe.

It was shown that by electrodeposition it is possible to obtain multilayers with high sensitivity, low GMR peak width, reduced coercivity and interesting GMR% values.

ACKNOWLEDGEMENTS

This work was supported by the European Community through BRITE-EURAM contract no. BRE-CT92-0342.

REFERENCES

1. M. N. Baibich, J. M. Broto, A. Fert, F. Nguyen Van Dau, F. Petroff, P. Etienne, G. Creuzet, A. Friederich and J. Chazelas; *Phys. Rev. Lett.* **61**, 2472 (1988).
2. D. S. Lashmore, Y. Zhang, S. Hua, M.P. Dariel, L. Swartzendruber, L. Salamanca-Riba; *Processes and Devices, Electrochem. Soc. Proc.* **94-6**, 205 (1994).
3. S. Lenczowski, C. Shö; *J. Magn. Magn. Mat.* **148**, 455 (1995).
4. M. Alper, W. Schwarzacher; *J. Electrochem. Soc.* **144**, 2346 (1997).
5. R. Hart, M. Alper, K. Altenborough, W. Schwarzacher; *Proc. 3rd Intern. Sympos. on Magn. Mat., Processes and Devices, Electrochem. Soc. Proc.* **94-6**, 215 (1994).
6. Y. Jyoko, S. Kashiwabara, Y. Hayashi; *J. Electrochem. Soc.* **144-1**, L5 (1997).
7. J. Yahalom, O. Zadok; *J. Mat. Sci.* **22**, 499-503 (1987).
8. D. Tench, J. White - *Metall. Trans.* A **15**, 2039 (1984).
9. D. S. Lashmore, M. P. Dariel; *J. Electrochem. Soc. Solid State and Technology* **133** (5) 1218 (1988).
10. N. Lecis, *PhD Thesis: "Leghe magnetiche a composizione modulata elettrodeposte"* Politecnico di Milano, IX Ciclo Torino (1997).
11. M. Alper, K. Attenborough, V. Barishev, R. Hart, D. S. Lashmore and W. Schwarzacher; *J. Appl. Phys.* **75**, 6543 (1994).
12. S. S. P. Parkin, Z. G. Li and D. J. Smith; *Appl. Phys. Lett.* **76**, 2710 (1991).
13. S. Z. Hua, D. S. Lashmore, W. Shwarzacher et al.; *J. Appl. Phys.* **76**, 6519 (1994).
14. W. Schwarzacher, D. S. Lashmore; *IEEE Transactions on Magnetics* **32**, 3133 (1996).

Table I: Bath compositions and plating conditions

	Bath 1 [mol/l]	Bath 2 [mol/l]	Bath 3 [mol/l]	Bath 4 [mol/l]
$Co\sigma_2$	0.04	0.05	0.04	0.04
$Ni\sigma_2$	0.02	0.025	0.02	0.02
$Cu\sigma_2$	0.006	0.005	0.006	0.006
$NaKC_4H_4O_6$	0.18	0.18	0.18	0.18
NaH_2PO_2	--	--	0.06	--
Thiocompound	--	--	--	5 ppm
$\sigma = NH_2SO_3^-$; pH = 6.40; T = 48°C; Stirring				

Table II: GMR measurements of two $[Cu(5nm)/CoNi(Cu)(3nm)]_{40}$ multilayers deposited onto Si+Cr(20nm) substrate in the absence and in the presence of a thin bright Ni ECD layer.

Bright Ni ECD layer	**GMR%**	**Middle Height Width [Oe]**	**Sensitivity [%/kOe]**	**Coercivity [Oe]**
No	3.45	180	25	90
Yes	4.06	230	35	49

Table III: GMR measurements of five multilayers grown onto different substrates.

ML Structure	**Substrate**	**Bath**	**GMR [%]**	**Sensitivity [%/kOe]**
$[Cu(5nm)/CoNi(Cu)(3nm)]_{40}$	B	1	5.0	45.9
$[Cu(5nm)/CoNi(Cu)(3nm)]_{40}$	D	2	6.9	48.8
$[Cu(5nm)/CoNi(Cu)(3nm)]_{40}$	E	2	5.4	41.1
$[Cu(7.5nm)/CoNi (Cu)(3nm)]_{40}$	D	2	6.8	34.0
$[Cu(7.5nm)/CoNi (Cu)(3nm)]_{40}$	E	2	5.7	55.8

Table IV: Comparison between GMR measurements of four $[Cu(5nm)/CoNi(Cu)(3nm)]_{40}$ multilayers electrodeposited in the presence (Bath4) and in the absence (Bath1) of thiocompound.

Samples	**Substrate**	**Bath**	**GMR [%]**	**Sensitivity [%/kOe]**	**Coercivity [Oe]**
I	C	1	3.5	25	90
II	C	4	5.7	70	65
III	B	1	5.0	46	45
IV	B	4	6.0	50	65

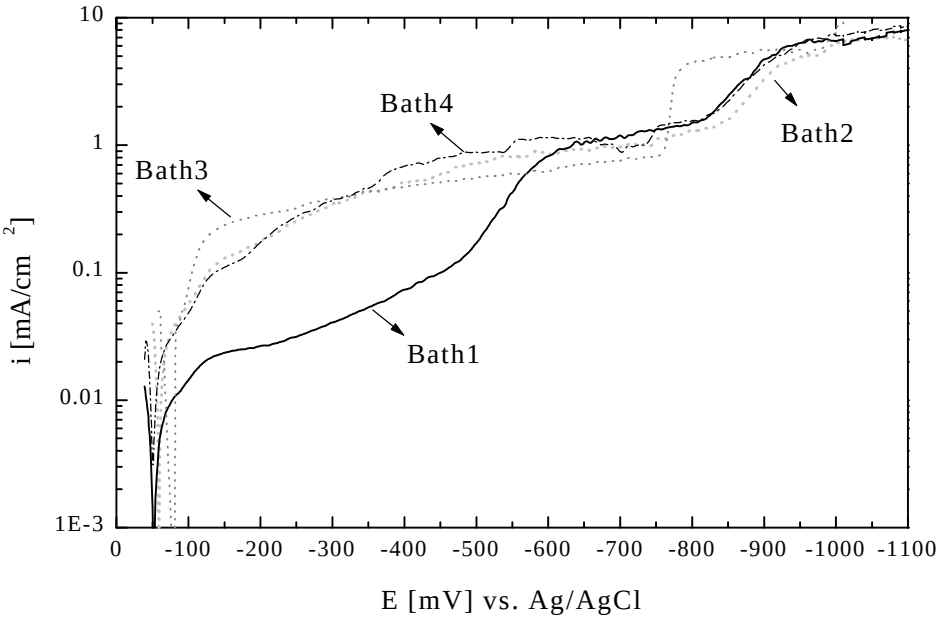

Figure 1: Polarisation curves for the different electrolytes

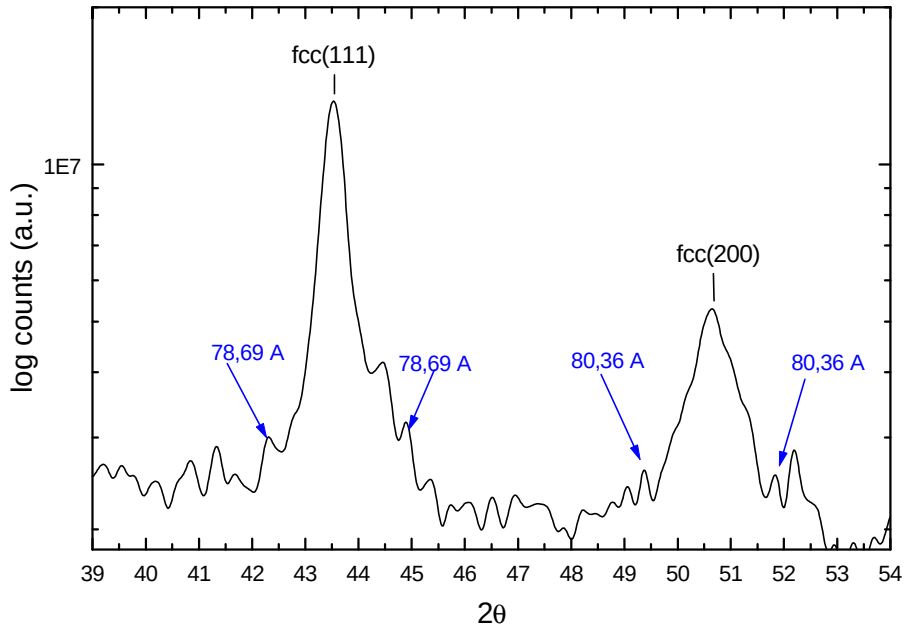

Figure 2: XRD pattern of a [Cu(5nm)/CoNi(Cu)(3nm)]$_{40}$ multilayer grown onto Si+Cr(20nm)+Au ECD flash (substrate C) in the presence of a thin Ni ECD film.

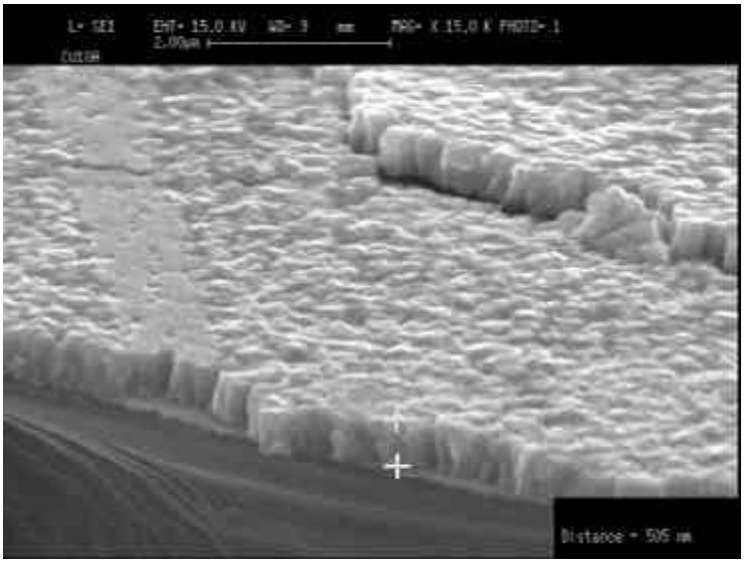

Figure 3: [Cu(5nm)/CoNi(Cu)(3nm)]$_{40}$ ML grown onto Si+Cr(20nm)+Au ECD flash (substrate C) SEM micrograph.

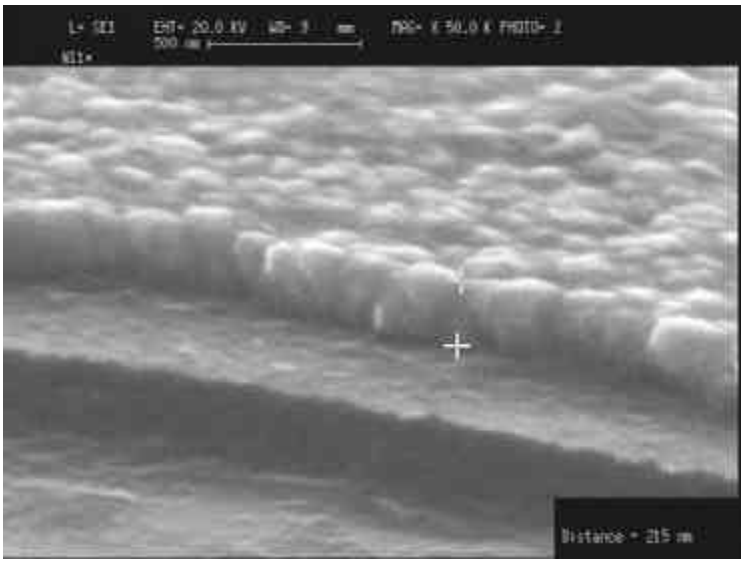

Figure 4: [Cu(5nm)/CoNi(Cu)(3nm)]$_{40}$ ML grown onto Si+Cr(20nm)+Au ECD flash (substrate C) in the presence of a thin bright Ni ECD layer.

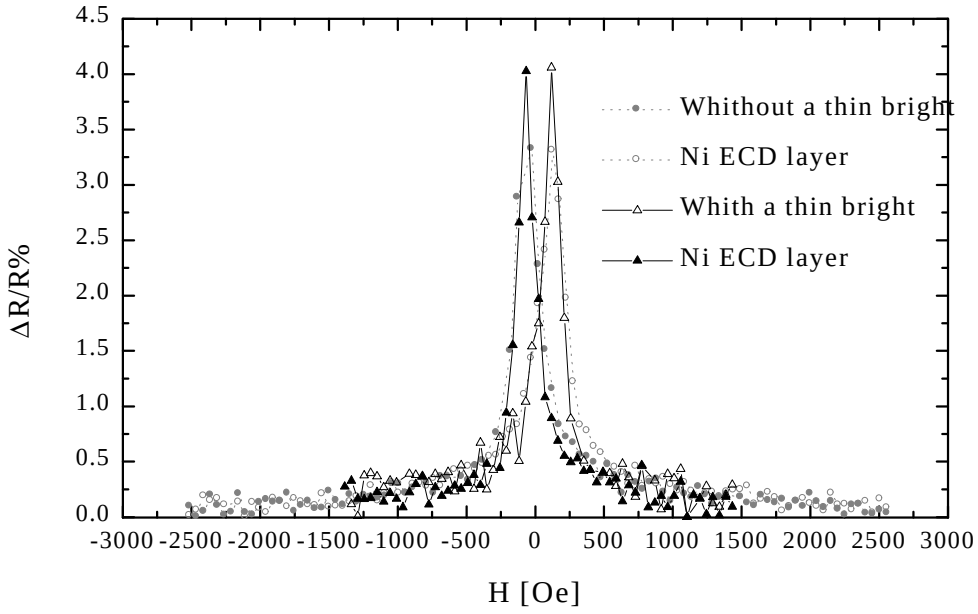

Figure 5: Two [Cu(5nm)/CoNi(Cu)(3nm)]$_{40}$ multilayers: the effect of a thin bright Ni layer electrodeposited on Si+Cr(20nm)+Au ECD flash (substrate C) on GMR curve.

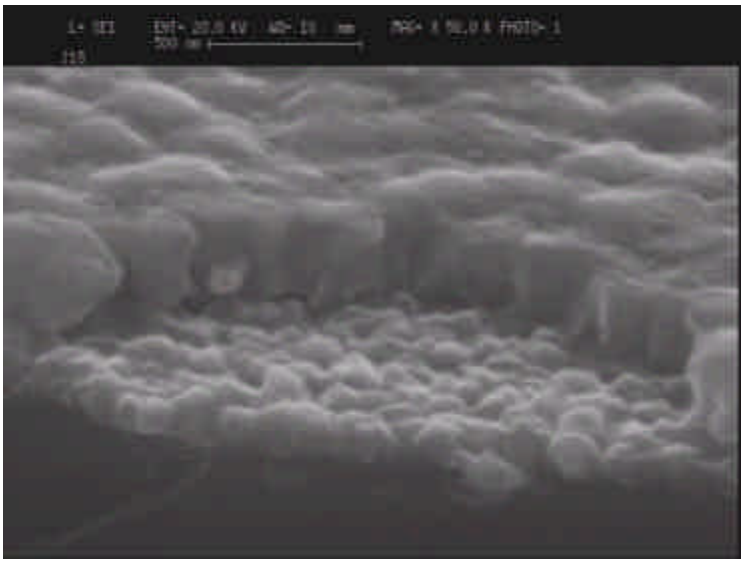

Figure 6: [Cu(7.5nm)/CoNi(Cu)(3nm)]$_{40}$ ML grown onto Si+ITO(160nm) (substrate D) SEM micrograph.

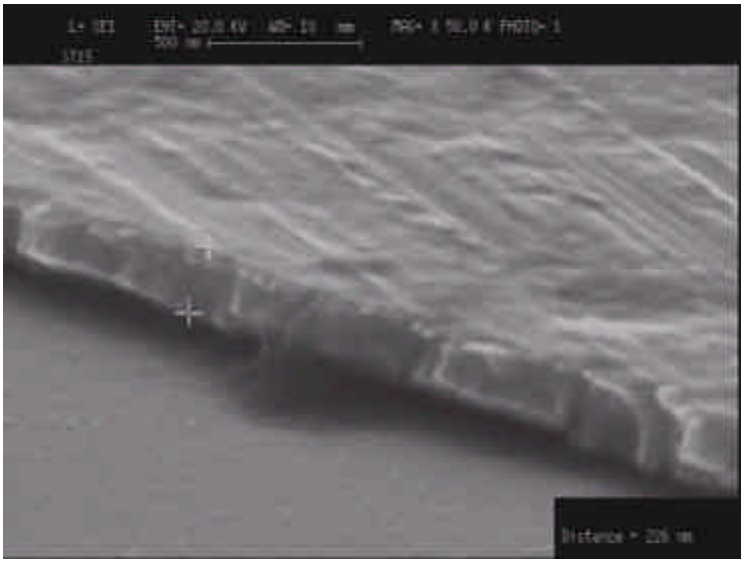

Figure 7: [Cu(7.5nm)/CoNi(Cu)(3nm)]$_{40}$ ML grown onto Si+SiO_2+Cr(70nm)+Au ECD flash (substrate E) SEM micrograph.

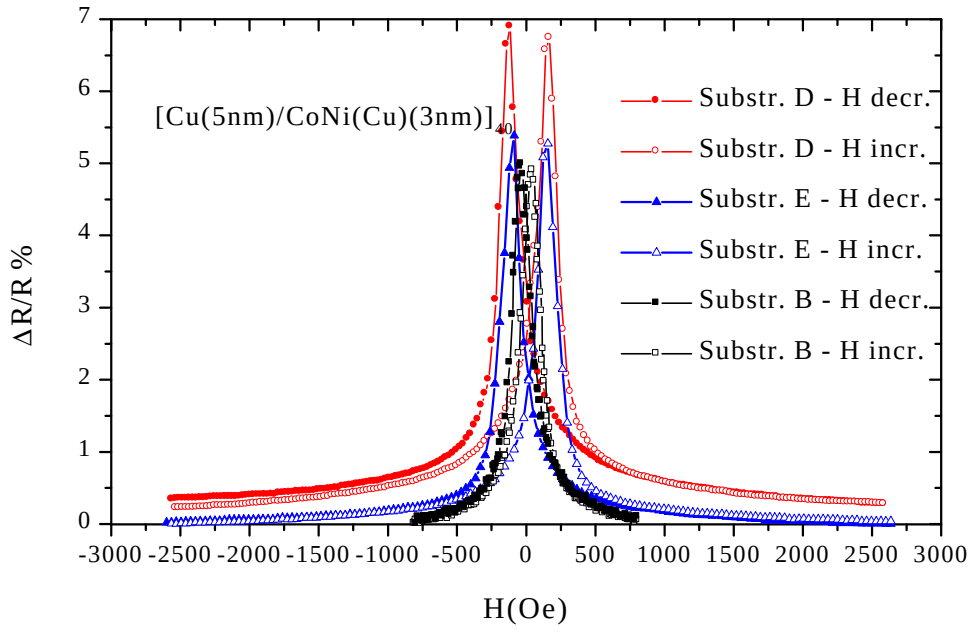

Figure 8: Three [Cu(5nm)/CoNi(Cu)(3nm)]$_{40}$ multilayers grown onto substrates B, D and E GMR curves.

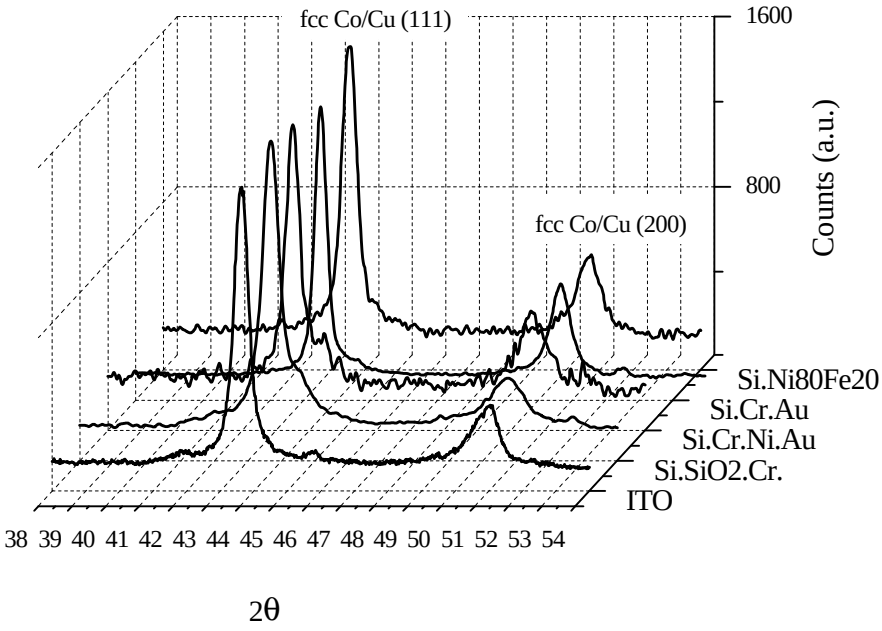

Figure 9: Five $[Cu(5nm)/CoNi(Cu)(3nm)]_{40}$ samples grown onto the following substrates: $Si+SiO_2(100nm)+Ni_{80}Fe_{20}$ (20nm); Si+Cr(20nm) with Au ECD flash; Si+Cr(20nm) with Au and bright Ni ECD flash; Si+ITO (*Indium Tin Oxide* -160nm) with Au ECD flash; $Si+SiO_2+Cr(70nm)$ with Au ECD flash XRD patterns.

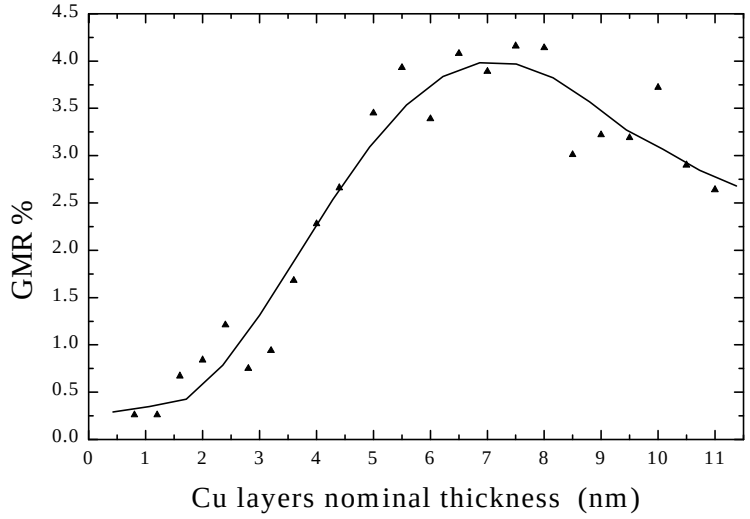

Figure 10: GMR% ratio as a function of Cu layer nominal thickness for MLs grown onto Si+Cr(20nm)+Au ECD flash (substrate C). The solid line is a guide to the eye.

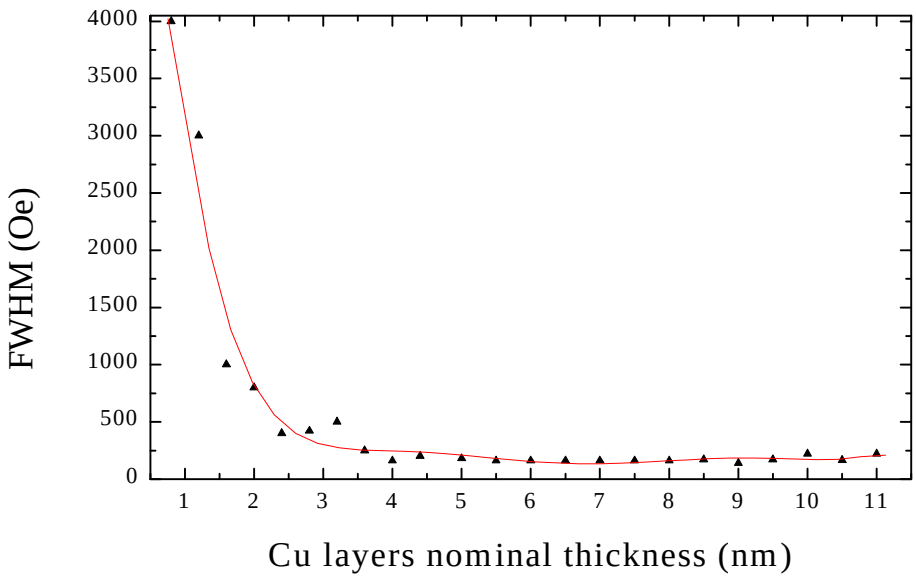

Figure 11: GMR peaks Middle Height Width as a function of Cu layer nominal thickness for MLs grown onto Si+Cr(20nm)+Au ECD flash (substrate C). The solid line is a guide to the eye.

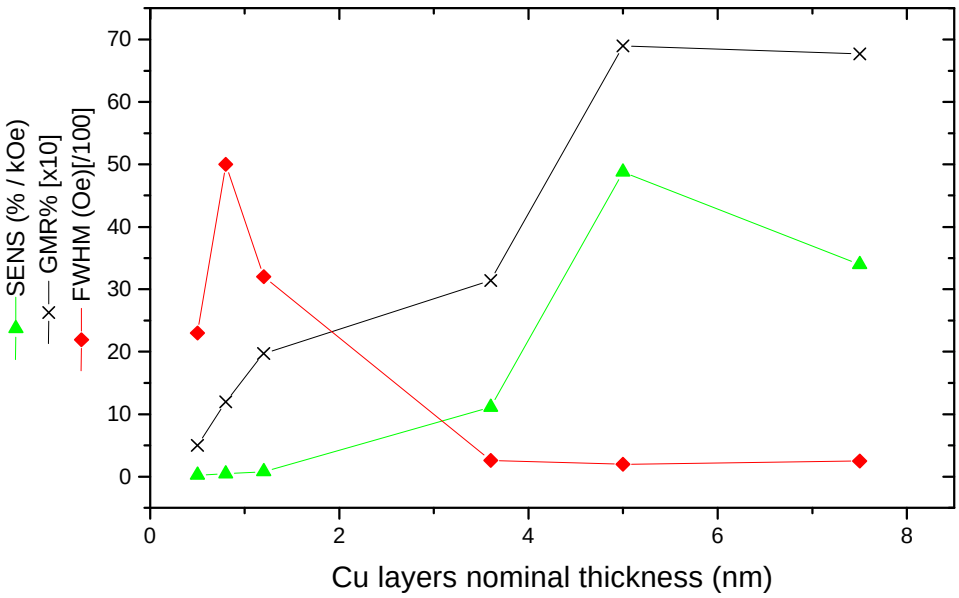

Figure 12: GMR%, FWHM and sensitivity as functions of nominal t_{Cu} for MLs grown onto Si+ITO(160nm) substrate. The solid lines are a guide to the eye.

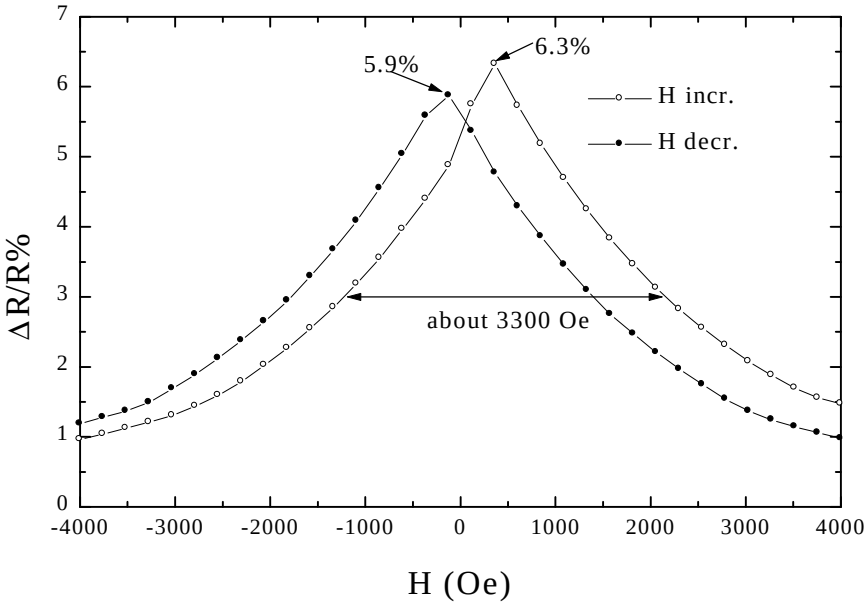

Figure 13: GMR curve of a $[Cu(1.2nm)/CoNi(Cu)(3nm)]_{255}$ Sample grown onto Si+Cr(20nm)+Au ECD flash (substrate C).

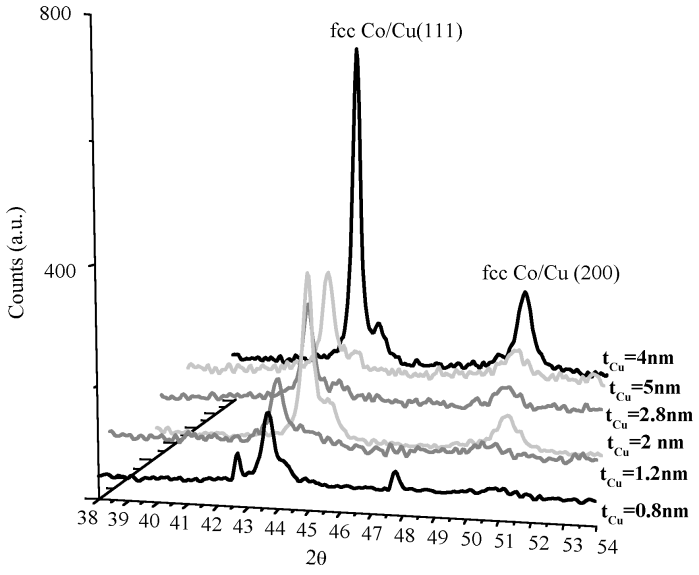

Figure 14: XRD patterns for six $[Cu(t_{Cu})/CoNi(Cu)(3nm)]_{40}$ samples grown onto Si+Cr(20nm)+ Au ECD flash (substrate C) at increasing nominal t_{Cu}.

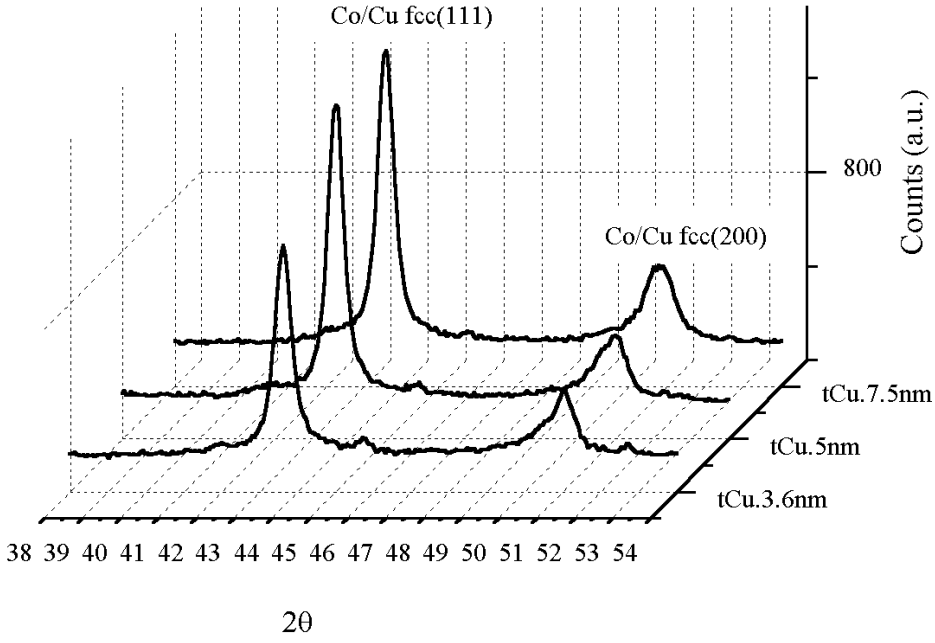

Figure 15: XRD patterns for three $[Cu(t_{Cu})/CoNi(Cu)(3nm)]_{40}$ samples grown onto Si+ITO(160nm)+Au ECD flash (substrate D) at increasing nominal t_{Cu}.

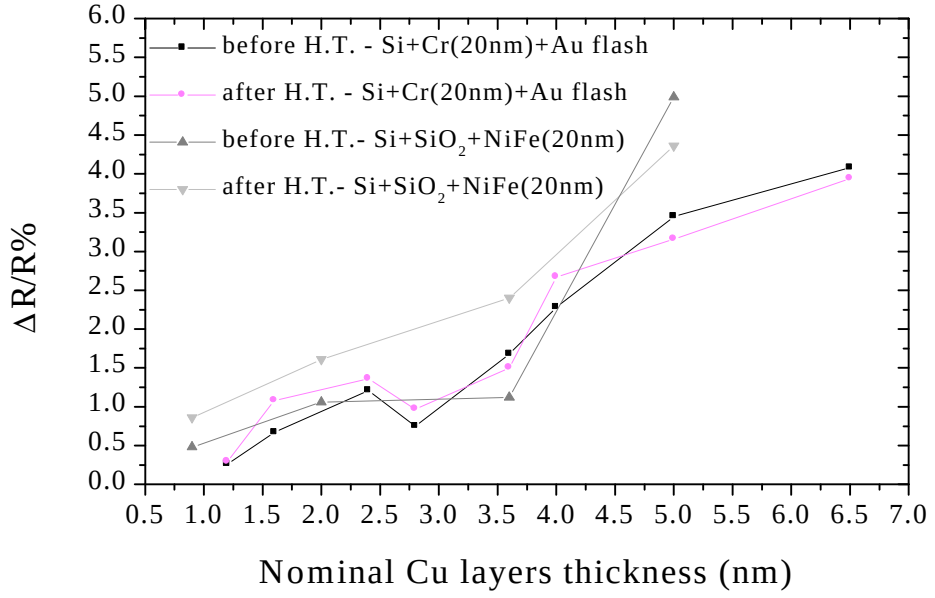

Figure 16: GMR% values at increasing t_{Cu} for multilayers grown onto substrates B and C before and after a 250°C-1h vacuum heat treatment.

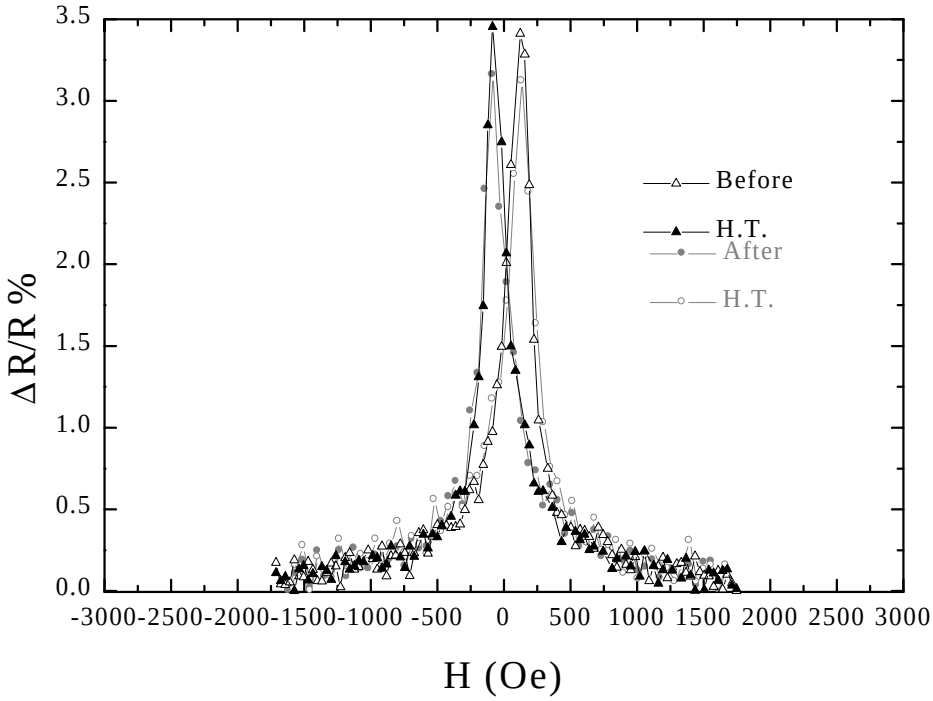

Figure 17: [Cu(5nm)/CoNi(Cu)(3nm)]$_{40}$ multilayer: comparison between GMR curves before and after 250°C 1h vacuum heat treatment.

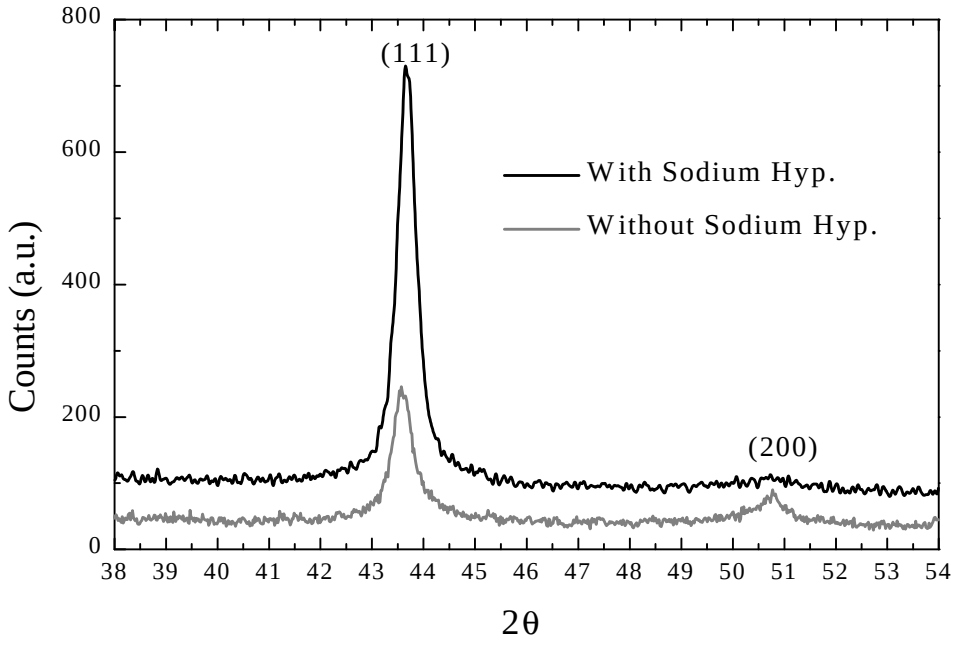

Figure 18: XRD patterns of two [Cu(2nm)/CoNi(Cu)(3nm)]$_{40}$ multilayers grown onto substrate B. The effect of Sodium Hypophosphite on their crystal structure.

Figure 19: SEM micrograph of a copper film electrodeposited from bath 1 at 0.5 mA/cm^2.

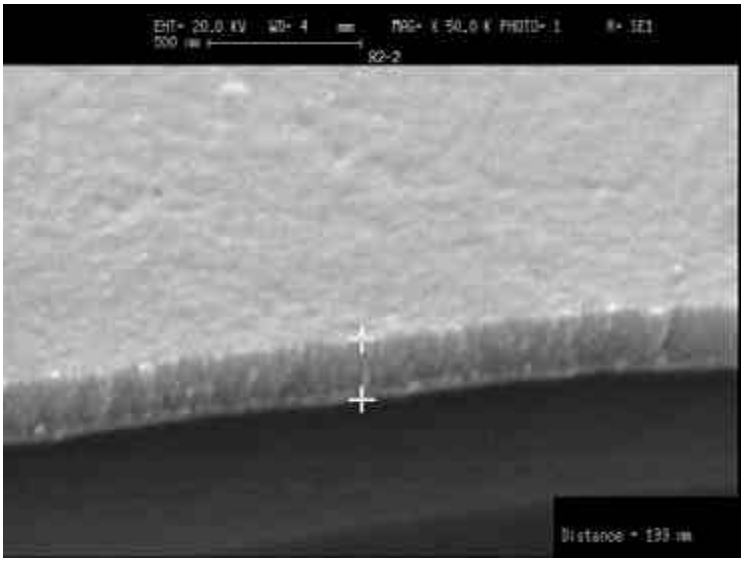

Figure 20: SEM micrograph of a copper film electrodeposited from bath 4 at 0.5mA/cm^2 in the presence of the thiocompound.

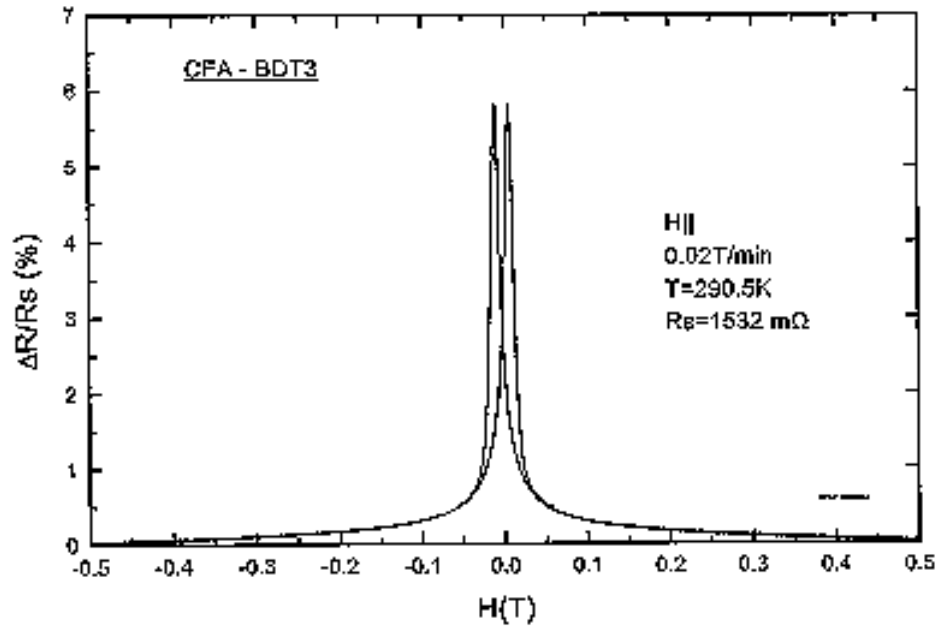

Figure 21: GMR curve of a [Cu(5nm)/CoNi(Cu)(3nm)]$_{40}$ multilayer electrodeposited onto Si+Cr(20nm)+Au ECD flash (substrate C) in the presence of thiocompound (bath 4), measured using Van Der Pauw technique. Sample II in table IV.

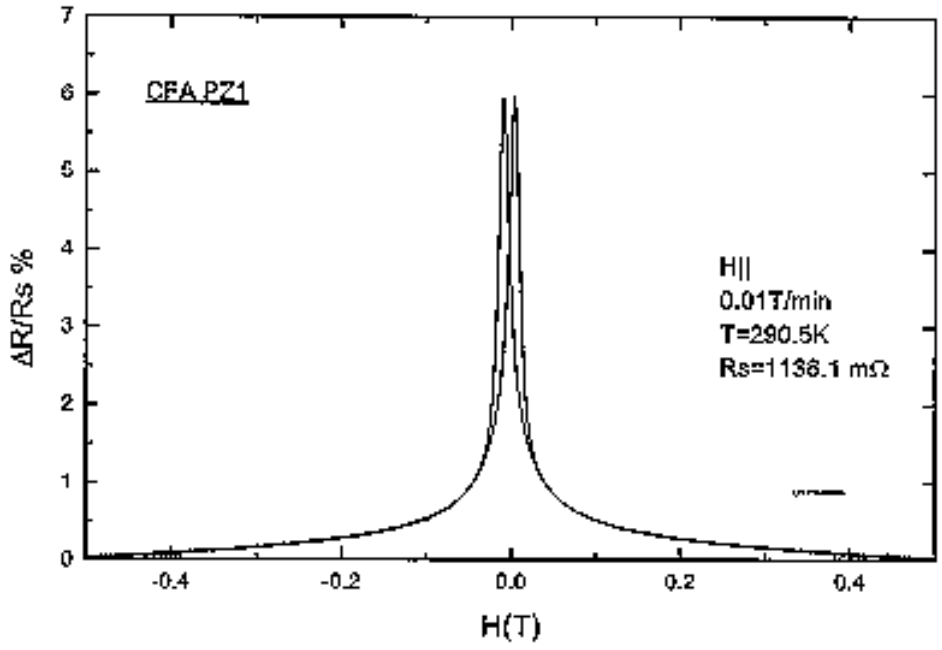

Figure 22: GMR curve of a [Cu(5nm)/CoNi(Cu)(3nm)]40 multilayer electrodeposited on substrate B in the presence of thiocompound (bath 4), measured using Van Der Pauw technique. Sample IV in table 4.